

# PHOTODISSOCIATION SPECTRUM OF CYANOBENZENE DIMER CATION. ABSENCE OF INTERMOLECULAR RESONANCE INTERACTION

KAZUHIKO OHASHI<sup>a</sup>, MASAHARU NISHIGUCHI<sup>a,b</sup>, YOSHIYA INOKUCHI<sup>a,b</sup>, HIROSHI SEKIYA<sup>b</sup> AND NOBUYUKI NISHI<sup>a,\*</sup>

<sup>a</sup>*Institute for Molecular Science, Myodaiji, Okazaki 444, Japan*

<sup>b</sup>*Department of Chemistry, Faculty of Science, Kyushu University, Hakozaki, Fukuoka 812-81, Japan*

## Abstract

Electronic spectra of a homo-molecular dimer cation,  $(\text{C}_6\text{H}_5\text{CN})_2^+$ , are measured by photodissociation spectroscopy in the gas phase. Broad features appeared in the 450–650 nm region are characteristic of  $\pi_3 \leftarrow \pi_{\text{CN}}$  transitions of the  $\text{C}_6\text{H}_5\text{CN}^+$  chromophore. No intense band is observed in the 650–1300 nm region, where other aromatic dimer cations usually show charge resonance bands. Two component molecules of  $(\text{C}_6\text{H}_5\text{CN})_2^+$  cannot take a parallel sandwich configuration suitable for the resonance interaction, because of geometrical constraints due to other stronger interactions.

---

\*To whom correspondence should be addressed.

## INTRODUCTION

A dimer cation is formed by the association of a radical cation with a neutral molecule of the same kind. The species is known to be important as a chemical intermediate for processes such as ion–molecule reactions, formation of larger cluster ions and ionic polymerization. A number of studies have long been made on the structure, stability and formation kinetics of dimer cations mainly in condensed phases [1–6] and also in the gas phase [7,8]. Optical measurement of dimer cations in condensed phases suffers a serious disadvantage; absorption bands of different cluster cations sometimes overlap on the spectra. Thus, there may be some ambiguity in identifying the species responsible for the photoabsorption. Recently, we have used mass-selected photodissociation spectroscopy to measure electronic spectra of dimer cations of benzene [9,10], toluene [11] and naphthalene [12] in the gas phase. The method has an advantage in that the size of the cations can be easily specified prior to the optical measurement. Two types of absorption bands are commonly seen on the spectra in the visible to near-infrared wavelength region. One is a charge resonance (CR) band, which arises from the resonance interaction between two component molecules of the dimer cation. The other is a local excitation (LE) band, which is due to an electronic transition of a monomer ion unit within the dimer. For each homo-dimer cation studied so far [9–12], the CR band is much stronger than the LE band. The result indicates that the two component molecules are equivalent to each other and that the positive charge is equally shared with the two molecules (charge delocalization). Since the CR band is due to the interaction between the  $\pi$  electron systems belonging to the two aromatic rings, a parallel sandwich structure is expected for these dimer cations rather than a T-shape structure. On the other hand, phenol dimer cation exhibits no strong CR band [13], although it is a homo-dimer cation. The result suggests that the two phenyl rings cannot be in a sandwich configuration suitable for the resonance interaction, owing to the geometrical constraint of an O–H $\cdots$ O hydrogen bond in  $(\text{C}_6\text{H}_5\text{OH})_2^+$ .

Neutral dimer and dimer cation of cyanobenzene are of interest because of its large dipole moment (4.14 D) [14]. The dipole–dipole interaction probably plays an important role in determining the geometry of the neutral dimer. Kobayashi and co-workers recorded laser-induced fluorescence (LIF) spectrum of  $(\text{C}_6\text{H}_5\text{CN})_2$  [15]. By comparing the observed

spectrum with the simulated one, they proposed a planar geometry for  $(\text{C}_6\text{H}_5\text{CN})_2$  with the two CN groups facing each other in an antiparallel configuration. Takayanagi and Hanazaki used fluorescence-dip spectroscopy to obtain vibrational spectra of  $(\text{C}_6\text{H}_5\text{CN})_2$  [16]. Recently, Ishikawa and co-workers measured stimulated Raman spectra of  $(\text{C}_6\text{H}_5\text{CN})_2$  and observed a single band for  $\nu_{12}$  vibration [17]. The result indicates that the dimer has a center of symmetry. This is consistent with the planar geometry proposed earlier [15]. If the neutral dimer does not undergo a large structural change upon ionization, then the two phenyl rings may be so far apart that the resonance interaction is insignificant in  $(\text{C}_6\text{H}_5\text{CN})_2^+$ .

In this article, we compare the photodissociation cross sections of  $(\text{C}_6\text{H}_5\text{CN})_2^+$  with those of  $(\text{C}_6\text{H}_6)_2^+$  in the CR band region. If  $(\text{C}_6\text{H}_5\text{CN})_2^+$  has a parallel sandwich structure like  $(\text{C}_6\text{H}_6)_2^+$ , the resonance interaction dominantly contributes to the binding energy of  $(\text{C}_6\text{H}_5\text{CN})_2^+$ . In such a case, we can expect the CR band of this cation with appreciable intensity. If other attractive effects, e.g. the presence of a  $\text{CN}\cdots\text{H}$  hydrogen bond or bonds, dominate over the resonance interaction, then the two component molecules may not take a sandwich configuration suitable for the resonance interaction. In this case, the CR band of  $(\text{C}_6\text{H}_5\text{CN})_2^+$  is expected to be much weaker than that of  $(\text{C}_6\text{H}_6)_2^+$ . The main subject of this work is to characterize the interaction between the two component molecules in  $(\text{C}_6\text{H}_5\text{CN})_2^+$ .

## EXPERIMENTAL

We applied the photodissociation spectroscopy to the mass-selected  $(\text{C}_6\text{H}_5\text{CN})_2^+$  ion in the gas phase. Tandem mass filter arrangements were employed, which isolated specific cluster ions for photodissociation and analyzed mass number of photofragment ions. We used two different methods to obtain the electronic spectra of  $(\text{C}_6\text{H}_5\text{CN})_2^+$ .

One method was based on the detection of the fragment ion. The measurement was carried out by using an apparatus with an octopole ion guide and two quadrupole mass filters [12,18]. Argon gas was bubbled through liquid cyanobenzene and the mixture was expanded through a pulsed nozzle. Cluster ions were produced by electron-impact ionization of neutral clusters formed in a supersonic expansion. The parent ion of interest was isolated through a quadrupole mass filter. After deflection by an ion bender, the ion beam was decelerated and

introduced into an octopole ion guide. A laser beam ( $\lambda_d = 340\text{--}780\text{ nm}$ ) propagated coaxially along the octopole and merged with the ion beam. Electronic excitation induced fragmentation of the parent ion. Mass number of the resulting fragment ions were analyzed by another quadrupole filter. After deflection by another ion bender, the ions were detected by a secondary electron multiplier. Only  $\text{C}_6\text{H}_5\text{CN}^+$  was detected as the fragment ion from  $(\text{C}_6\text{H}_5\text{CN})_2^+$  excited in the visible region. Therefore the photodissociation spectrum was obtained from the yield of  $\text{C}_6\text{H}_5\text{CN}^+$  as a function of wavelength of the laser.

The other method was the determination of the photodepletion efficiency of  $(\text{C}_6\text{H}_5\text{CN})_2^+$  relative to that of  $(\text{C}_6\text{H}_6)_2^+$  [13]. The measurement was carried out by using an apparatus with a reflectron-type time-of-flight (TOF) mass spectrometer [19]. A mixture of benzene and cyanobenzene seeded in argon was expanded through a pulsed nozzle. After passing through a skimmer and a collimator, the cluster beam entered the acceleration region of the mass spectrometer. An ionization laser beam ( $\lambda_i = 210\text{ nm}$ ) intersected the cluster beam, where the parent ions were produced by 2-photon ionization of neutral clusters. While traveling in the acceleration region, the parent ions were crossed by a dissociation laser beam ( $\lambda_d = 750\text{--}1300\text{ nm}$ ). After secondary acceleration, both the remaining parent ions and the photofragment ions were introduced into an ion-drift chamber of the mass spectrometer. The ions were then reflected by a two-stage ion reflector and detected by dual microchannel plates.

Figure 1 displays the dimer region of TOF mass spectra of the cluster ions produced from a mixture of benzene and cyanobenzene. The spectrum obtained without  $\lambda_d$  is shown in Fig. 1a. Three peaks at 45.8, 49.2 and 52.6  $\mu\text{s}$  correspond to  $(\text{C}_6\text{H}_6)_2^+$ ,  $(\text{C}_6\text{H}_6\cdots\text{C}_6\text{H}_5\text{CN})^+$  and  $(\text{C}_6\text{H}_5\text{CN})_2^+$ , respectively. The spectrum obtained with the dissociation laser ( $\lambda_d = 900\text{ nm}$ ) is exhibited in Fig. 1b. The laser beam irradiated the packets of the three ions simultaneously. Approximately 40 % of the  $(\text{C}_6\text{H}_6)_2^+$  signals disappeared by the introduction of  $\lambda_d$ . However, the depletion in the signals of  $(\text{C}_6\text{H}_6\cdots\text{C}_6\text{H}_5\text{CN})^+$  and  $(\text{C}_6\text{H}_5\text{CN})_2^+$  was less than 10 %. We confirmed that the behavior was *not* due to an incomplete overlap of the laser beam with the packets of  $(\text{C}_6\text{H}_6\cdots\text{C}_6\text{H}_5\text{CN})^+$  and  $(\text{C}_6\text{H}_5\text{CN})_2^+$ . The relation between the photodissociation cross section,  $\sigma(\lambda_d)$ , and the observed signal intensities is given by

$$\sigma(\lambda_d) \propto \ln[I_0 / I(\lambda_d)], \quad (1)$$

where  $I(\lambda_d)$  and  $I_0$  are the intensities of the parent ions detected with and without  $\lambda_d$ , respectively. From Eq. (1), the cross section for cyanobenzene dimer ion relative to that for benzene dimer ion is given by

$$\sigma_{\text{cyanobenzene}}(\lambda_d) = \sigma_{\text{benzene}}(\lambda_d) \frac{\ln[I_0 / I(\lambda_d)]_{\text{cyanobenzene}}}{\ln[I_0 / I(\lambda_d)]_{\text{benzene}}} . \quad (2)$$

Since we have already known  $\sigma_{\text{benzene}}(\lambda_d)$  as a function of  $\lambda_d$  [9,10], we can determine the value of  $\sigma_{\text{cyanobenzene}}(\lambda_d)$  from the measurement of the depletion efficiency.

## RESULTS AND DISCUSSION

### *Photofragment yield spectrum of $(\text{C}_6\text{H}_5\text{CN})_2^+$*

Figure 2 exhibits the spectrum of  $(\text{C}_6\text{H}_5\text{CN})_2^+$  in the region of 340–780 nm. The spectrum shows a prominent peak around 580 nm with a full width at half maximum of 15 nm. This feature lies on a much broader band extending from 450 to 650 nm. There is a small hump around 415 nm. The cross section gradually increases from 390 nm to shorter wavelength. No appreciable bands are seen in the 650–780 nm region. In order to interpret the spectrum, information on the electronic structure of  $\text{C}_6\text{H}_5\text{CN}^+$  is indispensable. To our knowledge, however, there is no report on the electronic spectrum of  $\text{C}_6\text{H}_5\text{CN}^+$  at least in the gas phase. The one-photon dissociation spectroscopy employed for  $(\text{C}_6\text{H}_5\text{CN})_2^+$  cannot be applied to  $\text{C}_6\text{H}_5\text{CN}^+$ , because the energy of a photon in the visible region is not enough to dissociate the monomer ion. A conventional method to obtain the spectrum for the ions of this kind is the use of weakly bound complexes with a rare gas atom [20]. Here, we measure the spectrum of  $(\text{C}_6\text{H}_5\text{CN}\cdots\text{Ar})^+$ . In this complex, the positive charge stays principally on the  $\text{C}_6\text{H}_5\text{CN}$  part because of its lower ionization energy. Since the binding energy of Ar to  $\text{C}_6\text{H}_5\text{CN}^+$  (less than 0.054 eV [21]) is much smaller than the electronic transition energy, electronic excitation of  $\text{C}_6\text{H}_5\text{CN}^+\cdots\text{Ar}$  and subsequent relaxation to lower electronic states result in the loss of the Ar atom. The appearance of the resulting  $\text{C}_6\text{H}_5\text{CN}^+$  is detectable by the mass spectrometry. Since the perturbation of the Ar atom to the  $\text{C}_6\text{H}_5\text{CN}^+$  chromophore is considered to be small, the spectrum of  $\text{C}_6\text{H}_5\text{CN}^+\cdots\text{Ar}$  mimics that of  $\text{C}_6\text{H}_5\text{CN}^+$ . Figure 3 displays the spectrum of  $\text{C}_6\text{H}_5\text{CN}^+\cdots\text{Ar}$  in the region of 430–630 nm. The most intense peak

is located at 522 nm with the second one at 514 nm. A group of weaker peaks are seen to the red of the primary maximum.

Photoelectron spectra of  $C_6H_5CN$  provide useful information on the energies for electronic states of  $C_6H_5CN^+$ . The adiabatic ionization energy was determined to be  $9.7315 \pm 0.0002$  eV by zero-kinetic-energy (ZEKE) photoelectron spectroscopy [21]. The ground electronic state of the ion is formed by removal of an electron from the  $\pi_3(b_1)$  orbital. The vertical ionization energies were reported to be 11.84 eV for a  $\pi_{CN}(b_2)$  electron, 12.09 eV for a  $\pi_{CN}(b_1)$  electron, 12.61 eV for a  $\sigma$  electron and 13.04 eV for a  $\pi_1(b_1)$  electron [22]. Thus the  $\pi_3 \leftarrow \pi_{CN}(b_2)$ ,  $\pi_3 \leftarrow \pi_{CN}(b_1)$ ,  $\pi_3 \leftarrow \sigma$  and  $\pi_3 \leftarrow \pi_1(b_1)$  transitions of  $C_6H_5CN^+$  are expected around 2.11, 2.36, 2.88 and 3.31 eV, respectively. The  $\pi_3 \leftarrow \pi_{CN}(b_2)$  transition is due to the promotion of an electron from the  $\pi_{CN}$  orbital in the plane of the phenyl ring, and it is dipole forbidden in  $C_{2v}$  symmetry. On the other hand, the  $\pi_3 \leftarrow \pi_{CN}(b_1)$  transition is an allowed transition, which is due to the excitation of an electron from the  $\pi_{CN}$  orbital perpendicular to the plane.

We can assign the most intense peak at 522 nm (2.38 eV) in the  $C_6H_5CN^+ \cdots Ar$  spectrum to the origin band of the allowed  $\pi_3 \leftarrow \pi_{CN}(b_1)$  transition. We tentatively attribute the weaker peaks at 548, 558 and 572 nm (2.26–2.17 eV) to vibronic bands of the forbidden  $\pi_3 \leftarrow \pi_{CN}(b_2)$  transition. The spectrum of  $(C_6H_5CN)_2^+$  exhibits broad features in the 450–650 nm region. These features are assigned to LE bands of the  $\pi_3 \leftarrow \pi_{CN}$  transitions of the monomer ion unit in  $(C_6H_5CN)_2^+$ . The small hump around 415 nm can be attributed to LE band of the  $\pi_3 \leftarrow \sigma$  transition, because  $\pi \leftarrow \sigma$  transitions are usually much weaker than  $\pi \leftarrow \pi$  transitions. The feature at wavelengths shorter than 390 nm is considered to be the tail of LE band of the  $\pi_3 \leftarrow \pi_1(b_1)$  transition.

#### *Photodepletion efficiency spectrum of $(C_6H_5CN)_2^+$*

The main purpose of this work is to examine whether the CR interaction is important to the binding energy of  $(C_6H_5CN)_2^+$ . The electronic spectrum in near-infrared wavelength region is helpful to understand the nature of the intermolecular interaction. The spectra of homo-dimer ions of benzene [9,10], toluene [11] and *p*-difluorobenzene [23] show intense CR

bands in this region. For each homo-dimer ion, the CR transition energy was found to be just twice of the binding energy, suggesting that the dominant contribution to the binding energy is from the resonance interaction [10]. If the resonance interaction between the two phenyl rings is also dominant in  $(\text{C}_6\text{H}_5\text{CN})_2^+$ , then we can expect a CR band of this ion with appreciable intensity.

Figure 4 displays the photodepletion spectrum of  $(\text{C}_6\text{H}_5\text{CN})_2^+$  in the region of 750–1300 nm. The closed circles were obtained from the depletion efficiency by using Eq. (2). The error bars indicate one standard deviation of statistical uncertainties determined from several sets of the measurement. The spectrum of  $(\text{C}_6\text{H}_6)_2^+$  is also shown by the broken curve for reference. At the wavelengths where the cross sections of  $(\text{C}_6\text{H}_6)_2^+$  are fairly large, we should reduce the power of the dissociation laser in order to avoid saturation; the experimental uncertainties are large in the 850–1000 nm region. Although weak features are seen in the region of 800–1050 nm, the cross sections of  $(\text{C}_6\text{H}_5\text{CN})_2^+$  are at most 10 % of the maximum cross section of  $(\text{C}_6\text{H}_6)_2^+$ .

The presence of the strong CR interaction in homo-dimer ions such as  $(\text{C}_6\text{H}_6)_2^+$  and  $(\text{C}_6\text{H}_5\text{CH}_3)_2^+$  strongly suggests a parallel sandwich configuration of the two aromatic rings in these ions. The configuration allows an overlap of  $\pi$  orbitals between the two rings, which is suitable for the CR interaction. On the other hand, the CR interaction is shown to be insignificant in  $(\text{C}_6\text{H}_5\text{OH})_2^+$  [13]. We propose that the two phenyl rings in  $(\text{C}_6\text{H}_5\text{OH})_2^+$  cannot be in a sandwich configuration owing to the geometrical constraint of an O–H $\cdots$ O hydrogen bond. The photodepletion behavior of  $(\text{C}_6\text{H}_5\text{CN})_2^+$  in the CR band region is similar to that of  $(\text{C}_6\text{H}_5\text{OH})_2^+$ . A geometrical constraint seems to be responsible for the absence of the CR interaction in  $(\text{C}_6\text{H}_5\text{CN})_2^+$  as well as in  $(\text{C}_6\text{H}_5\text{OH})_2^+$ . However, the geometry of  $(\text{C}_6\text{H}_5\text{CN})_2^+$  has not been determined yet. A planar geometry was proposed for  $(\text{C}_6\text{H}_5\text{CN})_2$  with the two CN groups facing each other in an antiparallel configuration [15]. Recently,  $(\text{C}_6\text{H}_5\text{CN})_2$  was shown to have a center of symmetry [17], which is consistent with the planar geometry proposed earlier [15]. If  $(\text{C}_6\text{H}_5\text{CN})_2$  does not undergo a large structural change upon ionization, then the two phenyl rings are so far apart that the CR interaction is insignificant in  $(\text{C}_6\text{H}_5\text{CN})_2^+$ . Even though the geometry of  $(\text{C}_6\text{H}_5\text{CN})_2^+$  is no longer a planar

one, the distance between the two rings must be much larger than that of  $(\text{C}_6\text{H}_6)_2^+$ , because the CR band of  $(\text{C}_6\text{H}_5\text{CN})_2^+$  is observed to be much weaker than that of  $(\text{C}_6\text{H}_6)_2^+$ .

The absence of the CR band suggests that the two phenyl rings in  $(\text{C}_6\text{H}_5\text{CN})_2^+$  cannot take a sandwich configuration. The antiparallel geometry of  $(\text{C}_6\text{H}_5\text{CN})_2$  is probably due to the large dipole–dipole interaction. In addition, the charge–dipole interaction contributes to the binding in  $(\text{C}_6\text{H}_5\text{CN})_2^+$ . The planarity of  $(\text{C}_6\text{H}_5\text{CN})_2$  is kept by the interaction between the electron-rich N atom and the electron-deficient *ortho*-H atom (CN $\cdots$ H hydrogen bond). The hydrogen bond is expected to become stronger on ionization. Actually, ZEKE spectroscopy of  $(\text{C}_6\text{H}_5\text{OH})_2$  suggested a significant strengthening of the O–H $\cdots$ O hydrogen bond on ionization [24]. In  $(\text{C}_6\text{H}_5\text{CN})_2^+$ , these effects dominate over the resonance interaction and prevent the two phenyl rings from taking a sandwich configuration.

Similar studies on dimer ions of *o*-, *m*- and *p*-dicyanobenzene will be of interest, because neutral dimer of *p*-dicyanobenzene was reported to have a parallel sandwich geometry [25].

## Acknowledgement

This work was supported in part by a Grant-in-Aid for Scientific Research (No. 09740450) from the Ministry of Education, Science, Sports and Culture of Japan.

## References

- [1] B. Badger, B. Brocklehurst and R. D. Russell, *Chem. Phys. Lett.* *1*, 122 (1967).
- [2] T. Shida and S. Iwata, *J. Chem. Phys.* *56*, 2858 (1972).
- [3] A. Kira, S. Arai and M. Imamura, *J. Chem. Phys.* *54*, 4890 (1971).
- [4] M. Itoh, *J. Am. Chem. Soc.* *93*, 4750 (1971).
- [5] M. A. Rodgers, *Chem. Phys. Lett.* *9*, 107 (1971).
- [6] H. Masuhara, N. Tamai, N. Mataga, F. C. De Schryver and J. Vandendriessche, *J. Am. Chem. Soc.* *105*, 7256 (1983).
- [7] M. Meot-Ner (Mautner), *J. Phys. Chem.* *84*, 2724 (1980).

- [8] K. Hiraoka, S. Fujimaki, K. Aruga and S. Yamabe, *J. Chem. Phys.* 95, 8413 (1991).
- [9] K. Ohashi and N. Nishi, *J. Phys. Chem.* 96, 2931 (1992).
- [10] K. Ohashi, Y. Nakai, T. Shibata and N. Nishi, *Laser Chem.* 14, 3 (1994).
- [11] Y. Inokuchi, K. Ohashi, T. Shibata and N. Nishi, to be published.
- [12] Y. Inokuchi, K. Ohashi, M. Matsumoto and N. Nishi, *J. Phys. Chem.* 99, 3416 (1995).
- [13] K. Ohashi, Y. Inokuchi and N. Nishi, *Chem. Phys. Lett.* 257, 137 (1996).
- [14] F. D. Lewis and B. Holman III, *J. Phys. Chem.* 84, 2326 (1980).
- [15] T. Kobayashi, K. Honma, O. Kajimoto and S. Tsuchiya, *J. Chem. Phys.* 86, 1111 (1987).
- [16] M. Takayanagi and I. Hanazaki, *J. Opt. Soc. Am. B* 7, 1898 (1990).
- [17] S. Ishikawa, T. Ebata and N. Mikami, to be published.
- [18] M. Matsumoto, Y. Inokuchi, K. Ohashi and N. Nishi, *J. Phys. Chem. A* 101, 4574 (1997).
- [19] K. Ohashi and N. Nishi, *J. Chem. Phys.* 95, 4002 (1991).
- [20] E. J. Bieske, M. W. Rainbird and A. E. W. Knight, *J. Phys. Chem.* 94, 3962 (1990).
- [21] M. Araki, S. Sato and K. Kimura, *J. Phys. Chem.* 100, 10542 (1996).
- [22] K. Kimura, S. Katsumata, Y. Achiba, T. Yamazaki and S. Iwata, *Handbook of HeI Photoelectron Spectra of Fundamental Organic Molecules*, Japan Scientific Societies Press, Tokyo, 1981. p. 196.
- [23] M. Fujii, K. Ohtsuka and M. Ito, unpublished results.
- [24] O. Dopfer, G. Lembach, T. G. Wright and K. Müller-Dethlefs, *J. Chem. Phys.* 98, 1933 (1993).
- [25] K. Fujita, T. Fujiwara, K. Matsunaga, F. Ono, A. Nakajima, H. Watanabe, T. Koguchi, I. Suzuka, H. Matsuzawa, S. Iwata and K. Kaya, *J. Phys. Chem.* 96, 10693 (1992).

## Figure Captions

Fig. 1. TOF mass spectra showing the photodepletion behavior of  $(\text{C}_6\text{H}_6)_2^+$ ,  $(\text{C}_6\text{H}_6 \cdots \text{C}_6\text{H}_5\text{CN})^+$  and  $(\text{C}_6\text{H}_5\text{CN})_2^+$  without the photodissociation laser (a) and with the laser at 900 nm (b).

Fig. 2. Photofragment yield spectrum of  $(\text{C}_6\text{H}_5\text{CN})_2^+$ . Intensities of the fragment  $\text{C}_6\text{H}_5\text{CN}^+$  ion are normalized by the dissociation laser power and plotted against the wavelength of the laser. Error bars indicate one standard deviation of statistical uncertainties determined from repeated laser scans.

Fig. 3. Photofragment yield spectrum of  $\text{C}_6\text{H}_5\text{CN}^+ \cdots \text{Ar}$ . Data points are obtained at intervals of 2 nm. Error bars are omitted for clarity.

Fig. 4. Photodepletion efficiency spectrum of  $(\text{C}_6\text{H}_5\text{CN})_2^+$ . Closed circles stand for the cross sections of  $(\text{C}_6\text{H}_5\text{CN})_2^+$  calculated by using Eq. (2) and scaled to the maximum cross section of  $(\text{C}_6\text{H}_6)_2^+$  at 920 nm. Broken curve is the spectrum of  $(\text{C}_6\text{H}_6)_2^+$  for reference.

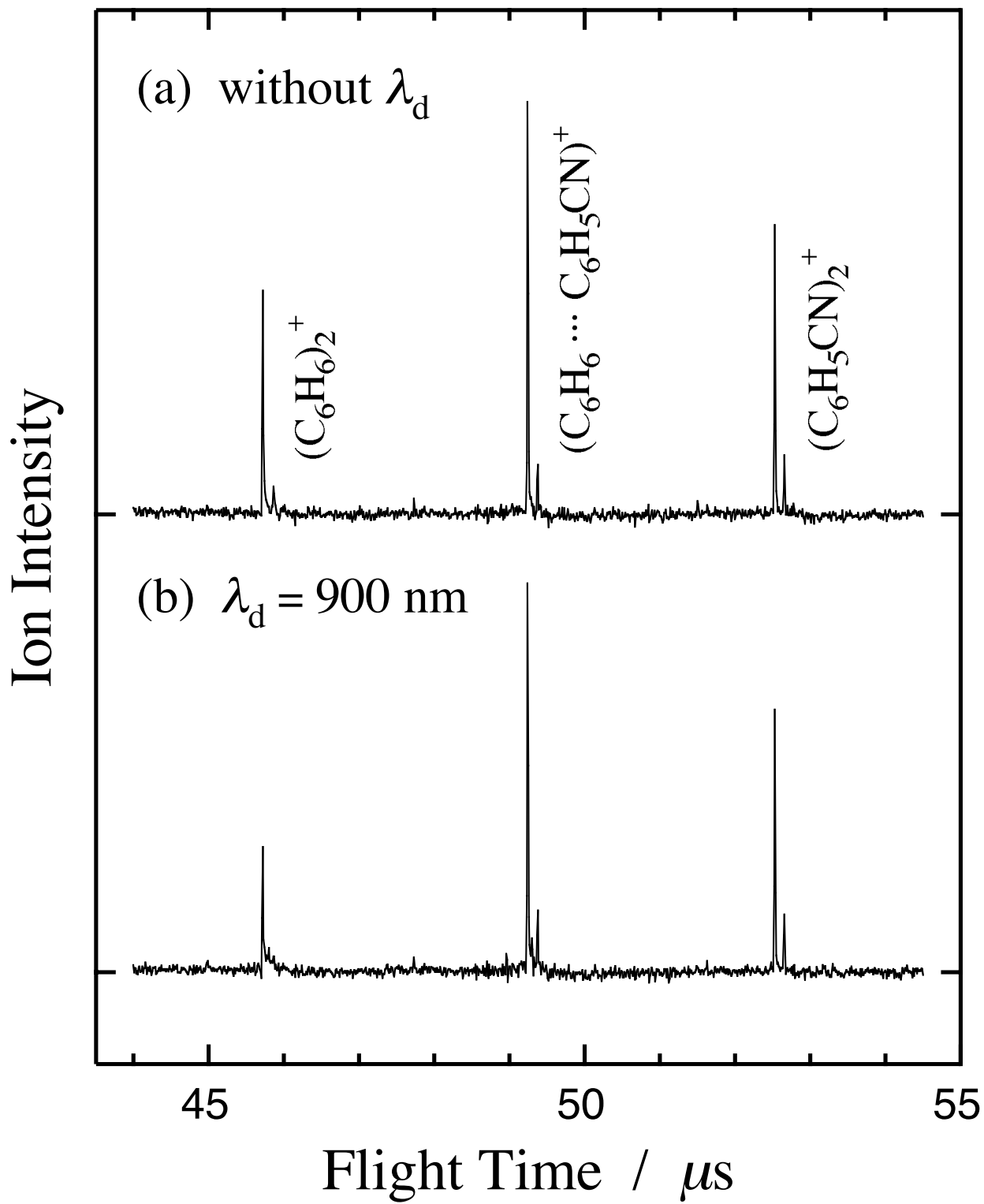


Fig. 1. Ohashi *et al.*

Cross Section (arb. units)

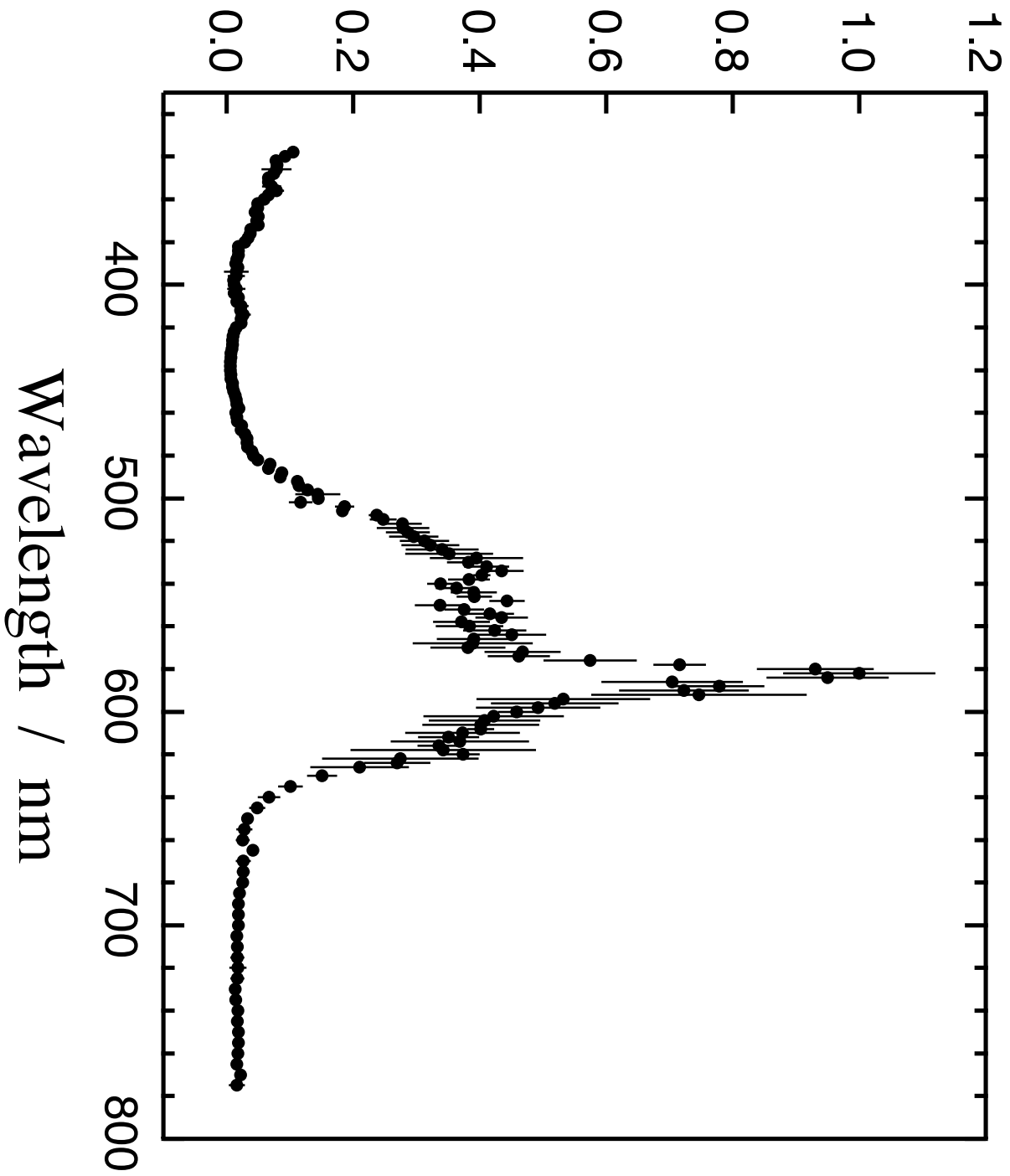


Fig. 2. Ohashi *et al.*

Cross Section (arb. units)

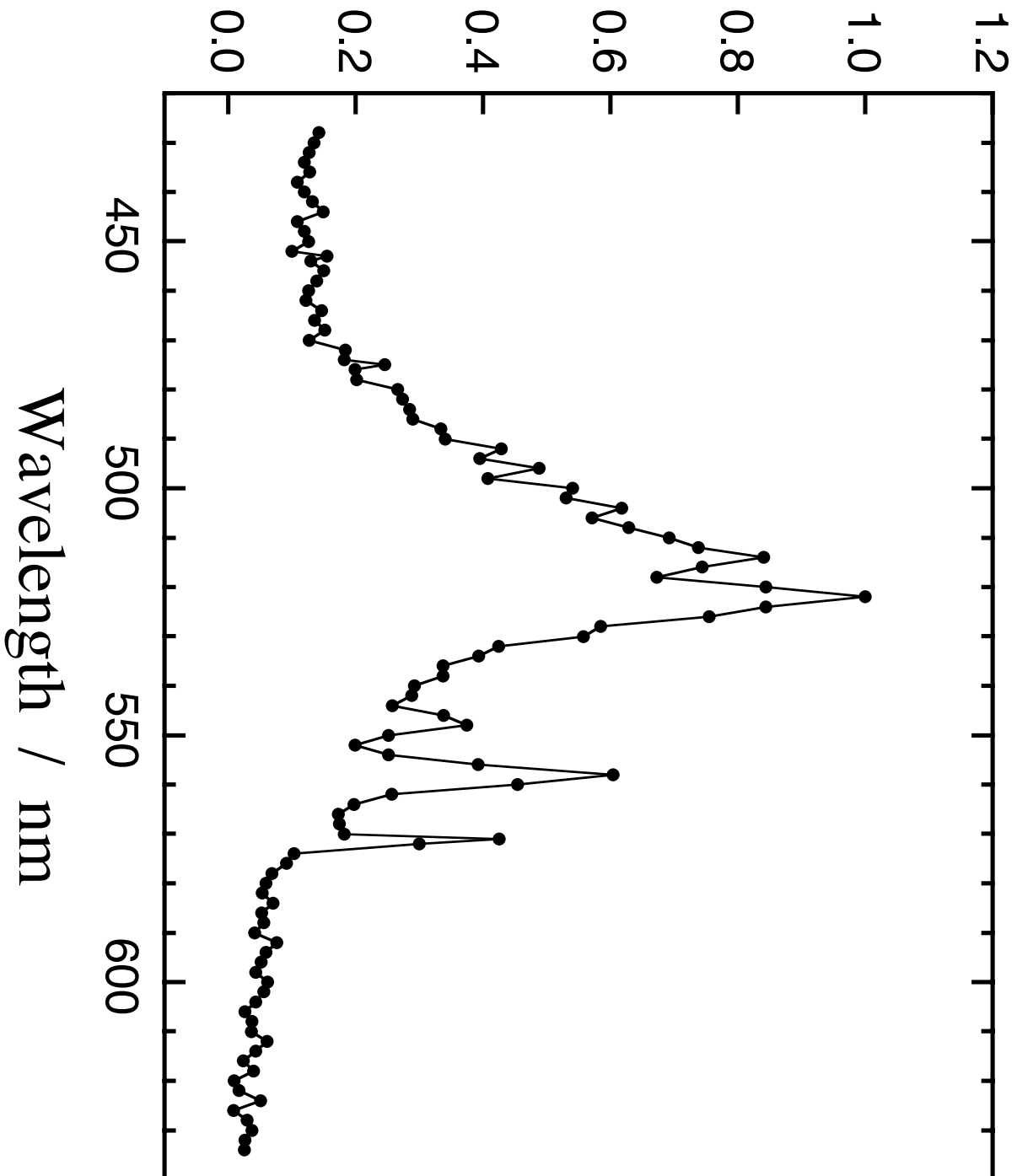


Fig. 3. Ohashi *et al.*

Fig. 4. Ohashi *et al.*

